Polymer Chemistry

Cellulose Nanocrystal-Reinforced Poly(5-triethoxysilyl-2-norbornene) Composites

Journal:	*Polymer Chemistry*
Manuscript ID	PY-ART-06-2019-000963.R1
Article Type:	Paper
Date Submitted by the Author:	10-Sep-2019
Complete List of Authors:	Hendren, Keith; Virginia Polytechnic Institute and State University, Materials Science and Engineering; Higgins, Morgan; University of Tennessee, Knoxville, Chemistry Long, Brian; University of Tennessee, Knoxville, Chemistry Foster, Johan; Virginia Polytechnic Institute and State University (Virginia Tech), Materials Science and Engineering

ARTICLE

Received 00th January 20xx,
Accepted 00th January 20xx
DOI: 10.1039/x0xx00000x

Cellulose Nanocrystal-Reinforced Poly(5-triethoxysilyl-2-norbornene) Composites

Keith D. Hendren,[a†] Morgan A. Higgins, [b†] Brian K. Long*[b] and E. Johan Foster*[a]

We demonstrate the reinforcement of a previously inaccessable norbornene-silane with a stiff, bio-based nanofiller. Poly(5-triethoxysilyl-2-norbornene) (PTESN), a glassy and thermally stable polymer, was combined with cellulose nanocrystals (CNCs) and solvent cast from toluene to form reinforced materials. Composite films showed excellent translucency and no visible aggregation, which was supported by scanning electron micrographs that showed no signs of CNC aggregation within the polymer matrix. Reinforcement was evident at moderate of 5 wt% CNC loading, showing a statistically significant enhancement for both Young's modulus (540 MPa vs 970 MPa) and storage modulus at 25 °C (400 MPa vs 1200 MPa). We suspect that there is a strong interaction between the polymer and CNC filler based upon the increase of thermal degradation temperature of the CNCs increasing, for example from 278 °C to 295 °C at 10 wt% CNCs. These interactions were probed via solid-state NMR, which suggests that no covalent bonding occurs between the triethoxylsilyl substituents of the polymer and the CNCs. We therefore hypothesize that hydrogen bonding interactions between PTESN and CNCs are responsible for the increased thermal stability and reinforcement of the polymer material.

Introduction:

Alkoxysilane-functionalized vinyl-addition polynorbornenes are an intriguing polymer class whose high molecular weight homopolymers were only recently accessed via careful catalyst selection (**Figure 1**).[1, 2] The prototypical vinyl-addition homopolymer poly(5-triethoxysilyl-2-norbornene) (PTESN) was preceded by other polymers with similar functionality, but that were made via ring opening metathesis polymerization (ROMP) to yield either rubbery[2] and glassy polynorbornenes[3] bearing trimethoxysilane or triethoxysilane pendant groups. However, PTESN films made via vinyl-addition are frequently more mechanically robust than their analogous ROMP polymers, which are often rubbery and exhibit tacky character.[2]

Cellulose nanocrystals (CNCs) are a unique filler material that has been previously incorporated into a wide variety of polymer matrices for reinforcement, through many different techniques such as solvent exchange,[4] melt mixing,[5] solvent casting,[6] and surface modification of CNCs.[6] CNCs are most commonly made into composite materials by dispersion into polar organic solvents, into which the polymer can also be dissolved and cast.[7] Another interesting and successful strategy of composite fabrication with CNCs and latex has been the emulsifying of the polymer into water and allowing the emulsified particles to interact with CNC particles.[8] Strategies for the incorporation of CNCs into a polymer matrix depend on the chemistry and morphology of the polymer.[9]

PTESN was previously characterized and shown to have moderate mechanical properties, making it an ideal prototype to expand the mechanical properties of this material class.[10] Therefore, reinforcement of this and other alkoxysilane substituted, vinyl-addition polynorbornenes will ultimately allow this class of materials to be used in much broader range of applications. As such, (CNCs) were chosen as an additive, as they possess an uncommon filler property of being largely transparent when well dispersed in addition to reinforcing polymer matrices.[11] Ideally, unfunctionalized CNCs are utilized

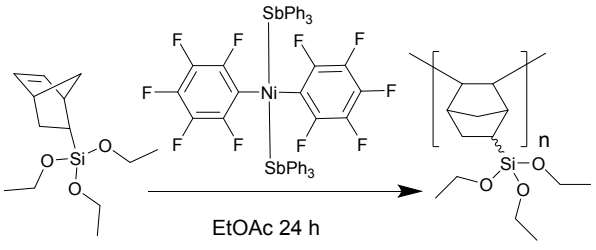

Figure 1. Vinyl-addition reaction scheme of PTESN synthesis with the catalyst trans-[$Ni(C_6F_5)_2(SbPh_3)_2$].

[a] Virginia Polytechnic and State University Materials Science and Engineering 445 Turner Street Blacksburg VA 24061
[b] University of Tennessee Department of Chemistry 1420 Circle Dr. Knoxville, TN 37996-1600
† Authors contributed equally to the manuscript
Electronic Supplementary Information (ESI) available: [details of any supplementary information available should be included here]. See DOI: 10.1039/x0xx00000x

in order to maximize hydrogen bonding interactions between CNCs and reinforce the host polymer. This reinforcement is generally more prevalent at higher CNC concentrations, as percolation networks can be formed under such conditions.[8]

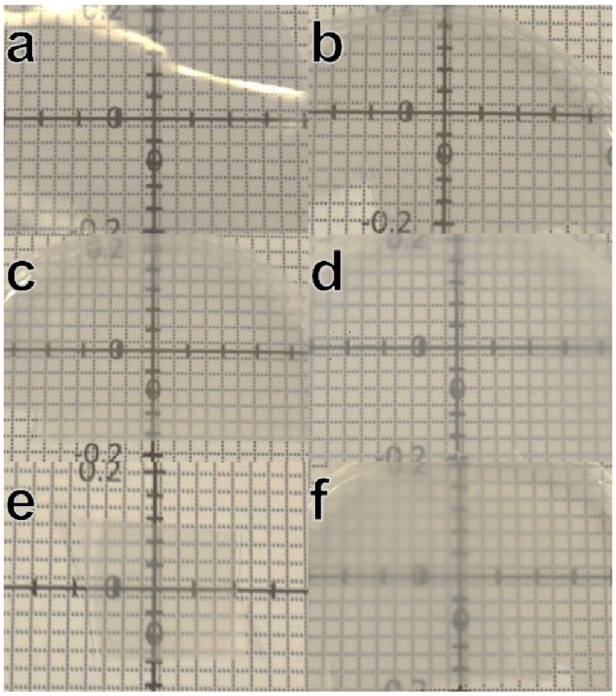

Figure 2. Optical photographs are arranged in order of increasing CNC content: **2a** PTESN, **2b** 1-CNC-PTESN, **2c** 5-CNC-PTESN, **2d** 10-CNC-PTESN, **2e** 15-CNC-PTESN, and **2f** 20-CNC-PTESN.

Previous efforts to reinforce alkoxysilane-bearing polymers using CNCs have focused on acrylate-based polymers and used CNCs as a platform for crosslinking.[12-19] Vinyl-addition polynorbornenes discussed here are distinct from those silane containing polymers that were combined with CNCs, such as trialkoxysilane functionalized polyacrylates, as they have a bicyclic backbone and form a rigid polymer without a need to use a crosslinking platform. Herein we show that we can easily fabricate CNC-PTESN composites that are dispersed by simple solvent casting from toluene. Confirmation of minimal aggregation was obtained from scanning electron microscope (SEM) and transmission electron microscope (TEM) imaging. Even at CNC concentrations as high as 20 wt% in PTESN (20-CNC-PTESN), TEM showed only very small as clusters of CNC aggregates. The dispersion was made more evident with mechanical reinforcement of the matrix polymer at high concentrations of filler loadings, illustrated by increases in the storage and Young's modulus, implying reinforcement from filler-filler and filler-matrix interactions. This work uses a novel polymer-filler system to study silane-OH interactions.

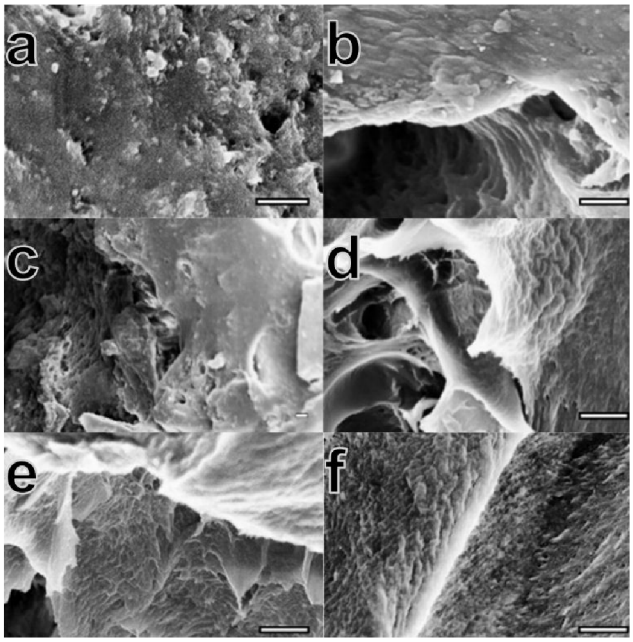

Figure 3. SEM micrographs are arranged in order of increasing CNC content. **3a** PTESN, **3b** 1-CNC-PTESN, and **3c** 5-CNC-PTESN, **3d** 10-CNC-PTESN, **3e** 15-CNC-PTESN, and **3f** 20-CNC-PTESN. All scale bars are 1 μm.

Results & Discussion:

The PTESN-CNC composite materials described herein are denoted as "#-CNC-PTESN" wherein the "#" represents the

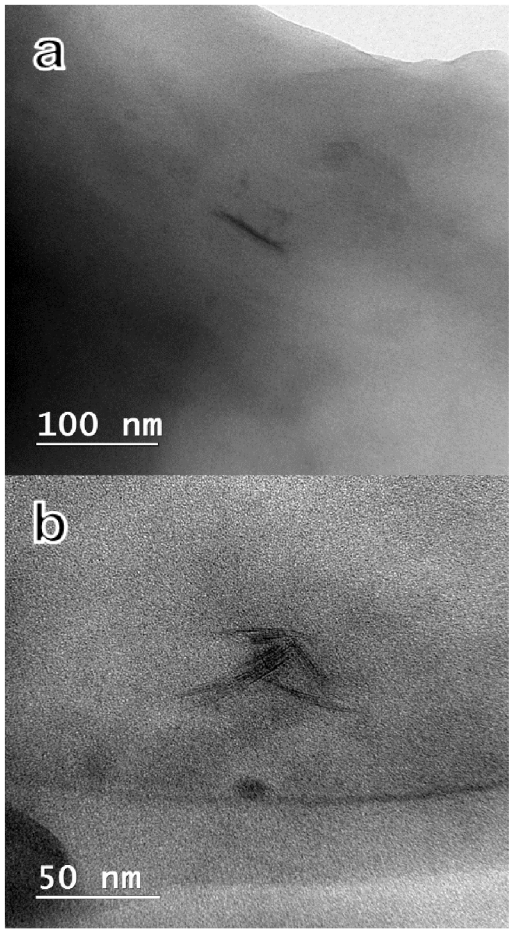

Figure 4. TEM of 20-CNC-PTESN shows occasional nanoscale aggregation of CNCs in PTESN composite films. The findings of occasional minor aggregation from images **4a** and **4b** suggest good dispersion.

wt% of CNCs dispersed in the composite material. Typically, dispersion of CNCs into a polymer matrix from solvent casting requires a polar organic solvent. However, as we will show, we found that CNCs could be readily dispersed in a PTESN matrix using toluene, a nonpolar solvent that fails to disperse unfunctionalized CNCs[20] without the aid of a surfactant.[21] These polymer solutions with CNCs could then be readily cast to yield CNC-PTESN composite films with apparent optical transparency when pressed against a field and possessing no macroscopically visible clusters or aggregates (**Figure 2**), despite toluene being a poor CNC dispersing solvent.[20] However, as expected the randomly oriented nanoparticles scatter visible light.

Observation with polarized optical microscopy did not show significant birefringence diagnostic of a liquid crystalline phase. SEM imaging used to examine the fracture surface of the composites found an absence of CNC aggregation on a 1-10 μm scale within cast films, suggesting that negligible amounts of CNC clusters were present at this scale. Further, the presence of nanosized features in PTESN **Figure 3a** made it exceedingly difficult to confirm the presence of dispersed CNCs in the other polymer films **Figures 3b-3f**. TEM imaging of these composite films did reveal the presence of some small clusters of aggregated CNCs within the polymer matrix (**Figure 4**). However, it should be noted that TEM imaging of individual CNCs within a carbon-based polymer matrix is exceedingly difficult[22] as the width of CNCs approach the resolution and contrast limits of TEM. This makes smaller clusters or individual CNCs difficult to image using this technique. As such, the lack of aggregated species on the macroscopic scale (**Figure 2**) and the lack of significant aggregation via TEM imaging (**Figure 4**) suggest that there is a good dispersion of CNCs within the matrix, though the authors acknowledge this is not definitive proof of ideal CNC dispersion.

The DMA data indicates that storage modulus E' is increased at CNC concentrations as low as 5 wt%, and steadily increases as a function of CNC loading percent starting at an initial value of 400 MPa for PTESN and ending with a value of 1200 MPa for PTESN-20-CNC at 25 °C (**Table S1**). It should be noted that the applications available for a polymer with a storage modulus of 1200 MPa are significantly broader than those applicable to non-reinforced PTESN, thereby opening the use of these nanocomposites to a broader audience.

Representative tan δ curves (**Figure 5**) show a shift in the glass transition temperature of the composite material indicating strong interactions between filler and matrix.[23] Further, broadening is observed which has been ascribed to the loss of mobility of the polymer chains through the possible mechanisms of friction from filler particle interactions, filler polymer motion at filler interface, or a change in polymer properties at filler interface.[23, 24]

Young's modulus increases as CNC loading is increased, and significant enhancements are observed at 5 wt% CNC loading increasing from the neat polymer at 540 MPa to 700 MPa and further increased for 20-CNC-PTESN to 970 MPa. The strain at break and toughness have a trend of decreasing toughness and elongation at break with increased CNC loading. In contrast there is not a clear trend with the change in maximum tensile stress as the experimental error of the neat PTESN and 1-CNC-PTESN. Data from **Table S2** and representative curves (**Figure S3**) show these trends.

Thermal gravimetric analysis of these composites revealed an increase in the thermal degradation temperature of the CNCs

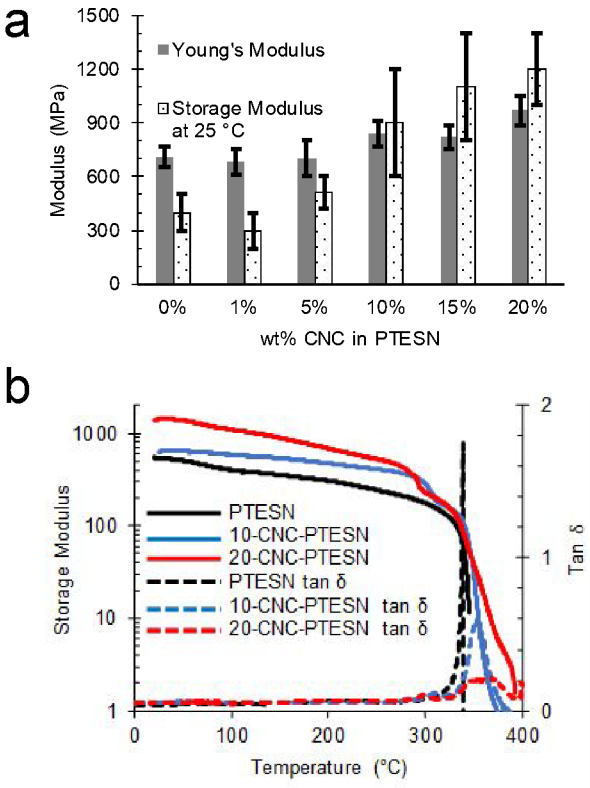

Figure 5. PTESN CNC composites were tested with dynamic mechanical analysis (DMA) and tensile testing. Reinforcement from increased stiffness (E' and E) is presented on bar graph **5a** and DMA traces show the increase in storage modulus (E') with increasing CNC content **5b**.

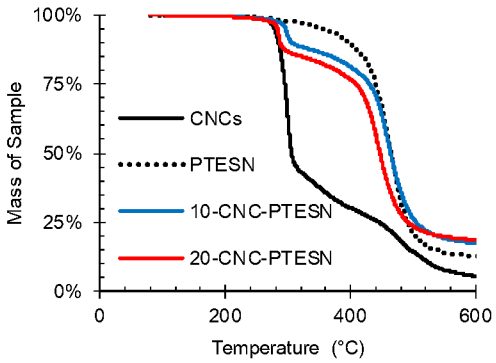

Figure 6. Thermogravimetric analysis of neat CNCs, 10-CNC-PTESN, 20-CNC-PTESN, and PTESN show that the CNCs have increased thermal stability when combined with PTESN. The 5 wt% loss for neat CNCs is ca. 278 °C, 10-CNC-PTESN is ca. 295 °C, and 20-CNC-PTESN is ca. 283 °C, and PTESN is 354 °C.

°C 15-CNC-PTESN, and 283 °C for the 20-CNC-PTESN sample (**Figure 6**). Notably 1-CNC-PTESN and 5-CNC-PTESN do not have a clear degradation event associated with CNCs. Previous studies have hypothesized that there is an increase in thermal stability of cellulose composite materials when there are favourable interactions between the filler and matrix arising from van der Waals interactions and hydrogen bonding, and a decrease in thermal stability upon aggregation of the cellulose filler.[23] Application of this relationship could correspond to a 10-CNC-PTESN that is well dispersed and thermally stabilized and for 15-CNC-PTESN and 20-CNC-PTESN samples approach the onset of aggregation for the material. Data for all TGA traces is available as **Figure S4**.

Previous polymers that have been able to increase the degradation temperature of CNCs include polyvinyl alcohol,[25] polyfuryl alcohol (PFA),[26] and γ-aminopropyltrimethoxysilane (APS) functionalized CNCs in polyurethane.[15] Interestingly, the PFA-CNC composite showed great thermal stability and its (C-O-C) backbone is analogous to PTESN's pendant groups (Si-O-C) as only being able to accept hydrogen bonds. Additionally, APS functionalized CNCs mixed with polyurethane are interesting as the trimethoxysilane functional groups on the CNCs may have similar interactions as the CNC-PTESN composite system studied herein.

To better understand how and why we are able to readily disperse CNCs in a PTESN matrix using a typically poor performing solvent, toluene, we looked to a previous study that explained favourable interactions between alkoxylsilane molecules and cellulose fibers.[13] This study suggested that alkoxysilane groups are subject to reactions with alcohols and adventitious water to form silanol groups (Si-OH). Furthermore, previous studies have shown that cellulose may form covalent bonds with these pendant side groups (Si-O-cellulose) and residual moisture may lead to possible siloxane linkages (Si-O-Si) under similar conditions.[13, 27] In our study, solid-state NMR (^{29}Si and ^{13}C) was employed to interrogate both the PTESN and 20-CNC-PTESN systems (**Figure 7**).

The ^{29}Si NMR spectra for PTESN and 20-CNC-PTESN are shown in Figure 7 in which both samples showed only a single resonance indicating that there is no detectable amount of hydrolysis (Si-OH) or etherification reactions (Si-O-Si) occurring. Previous studies that have found additional peaks further upfield ca. 7-9 ppm for self-condensed (Si-O-Si) etherification bonds and hydrolysis (Si-OH).[13, 27] These studies were unable to directly detect the presence of (Si-O-) groups bonded to cellulose as there likely not an appreciable change in chemical shift. The solid-state ^{13}C spectrum of the 20-CNC-PTESN, has peaks are similar to previous ^{13}C spectra of the neat polymer[1] with expected peaks from cellulose.[28] Although this is not conclusive, as we believe the number of reactions, if any are occurring, are below the detection limit of NMR, and we do not discount the possibility of hydrolysis reactions. Although water was not directly added to the system, atmospheric water did have ample opportunity to react with the PTESN and 20-CNC-PTESN, however, there is no evidence of hydrolysis occurring in **Figure 7**. As water is more reactive than primary ether species (C-OH) we believe that (Si-O-CNC) linkages are unlikely.

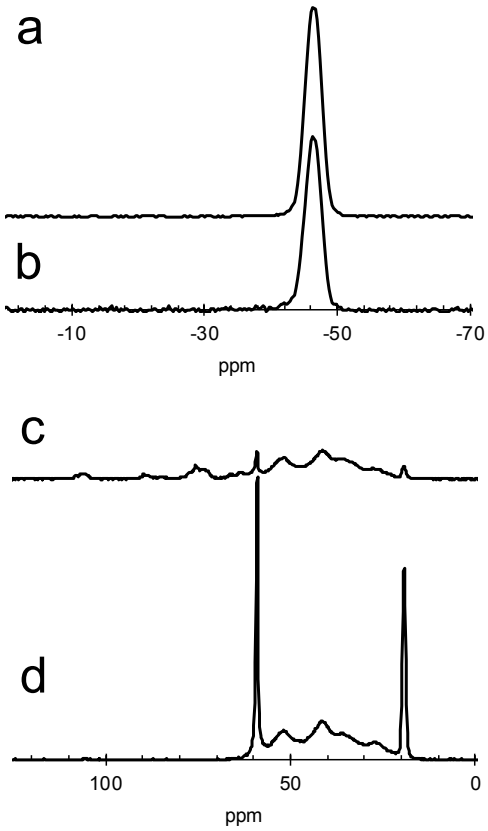

Figure 7. Solid-State NMR spectra of PTESN and 20-CNC-PTESN with the number of scans noted in parenthesis. The ^{29}Si NMR spectra for **7a)** neat PTESN (2000) and **7b)** 20-CNC-PTESN (32000). The ^{13}C spectra of **7c)** neat PTESN (8000) and **7d)** 20-CNC-PTESN (8000), respectively.

Hydrolysis reactions creating (Si-OH) groups would likely improve interactions between the CNCs and the pendant groups, which would then act as strong hydrogen bond acceptors and donors for the numerous hydroxyls displayed on the CNCs. The significant reinforcement observed indicates that some advantageous interactions between the polymer and filler are present and based upon the spectral data collected we hypothesize that hydrogen bonding between the CNCs and the Si-O-R moieties, with or without water, are the most likely sources of these favourable interactions.

Experimental

Materials

The catalysts trans-[Ni(C_6F_5)$_2$($SbPh_3$)$_2$] and monomer 5-triethoxysilyl-2-norbornene were synthesized according to literature procedures.[1, 10] Ethyl acetate (EtOAc) was dried over CaH_2 and degassed via three freeze-pump-thaw cycles. All polymerizations were conducted in a glovebox under air-free conditions unless otherwise noted. Solution-state NMR

spectroscopy was conducted using a Varian Mercury Vx 300 MHz instrument and referenced to residual solvent. Wood CNCs hydrolysed from sulfuric acid with 0.94% sulphur content by weight and dimensions of 90 ± 40 nm by 7 ± 2 nm (**Figure S5**) were obtained from the University of Maine Forest Products Laboratory and dried overnight at 50 °C under high vacuum before use.

Synthesis of poly(triethoxysilylnorbornene) (PTESN)

Polymerizations were conducted using a modified literature procedure.[1, 10] In a typical polymerization, the catalyst *trans*-$[Ni(C_6F_5)_2(SbPh_3)_2]$ (0.011 g, 10 μmol) was added to a stirred solution of ethyl acetate (EtOAc) (4 mL) and the monomer 5-triethoxysilyl-2-norbornene (2.56 g, 10 mmol). The polymerization was stirred for 24 h, then diluted with additional EtOAc (6 mL) and precipitated into excess methanol (**Figure 1**). The resultant polymer was isolated via vacuum filtration and dried *in vacuo* to yield PTESN (1.359 g, 53.1%, Mn 227 kg/mol, and Đ 2.18), which was characterized by NMR (**Figure S1**) and GPC (**Figure S2**). The dispersity agrees with the ranges previously published for vinyl-addition polymerizations.[1]

Gel Permeation Chromatography (GPC)

Molecular weight data for PTESN was measured using a Tosoh EcoSEC GPC operating at 40 °C in THF and molecular weight values are reported relative to polystyrene standards.

Fabrication of CNC-reinforced PTESN films

CNCs were dried by heating at 50 °C under vacuum for 12-24 h. PTESN (0.5 g) was dissolved in toluene (10 mL) and pushed through 0.45 μm PTFE syringe filter into a clean vial. The dried CNCs (1-20 wt%) were added to the polymer solution, capped, and the resultant suspension stirred for 48 h. The suspension was then deposited onto a levelled Teflon casting dish, covered with aluminium foil, and the solvent slowly evaporated for 5 days. Recovered samples are referenced using the #-CNC-PTESN format in which # represents the wt% of CNCs relative to PTESN.

Dynamic Mechanical Analysis

Dynamic mechanical analysis was conducted using a TA Instruments Q800 DMA using a film tension clamp and a temperature ramp from room temperature to 400 °C at 0.1% strain, 1 Hz, and a heating rate of 5 °C/min. Tested films were cut into rectangular coupons that were ca. 5 mm in width, 15 mm in length, and ca. 150 μm thick.

Tensile Testing

Tensile tests were run on an Instron 5943 with a strain rate of 1 mm/min. The sample dimension of the dog bone specimens were ca. 110 μm thick and 3.5 mm wide with a gauge length of ca. 15 mm.

Scanning Electron Microscopy

PTESN and all CNC-PTESN composite films were fractured by bending the films to a 180° angle and gently pulling the two pieces apart. Films were placed on aluminium SEM holders on double stick carbon tape and oriented into a beach chair configuration and coated with 5 nm of iridium in a Leica Sputter Coater. Images of the fractured surface were taken using a Zeiss Leo Gemini SEM In-lens detector.

Transmission Electron Microscopy

The 20-CNC-PTESN composite film was mounted on an SEM holder with folded single sided copper tape and coated with 5 nm of iridium using a Leica sputter coater. The sample was flipped, and the other side coated with another 5 nm of iridium. The sample was then embedded in epoxy and cut into 125 nm sections using a Diatome diamond knife on an RMC microtome with water at room temperature. Sample was retrieved from the microtome using the perfect loop method and a 300 mesh Peclo formvar coated lacey grid, which was then imaged using a JEOL 2100 TEM.

Solid State NMR

Solid state ^{13}C and ^{29}Si NMR spectra were collected using a Bruker III 600 MHz NMR at 2000-32000 scans to analyse samples for a silyl ether reaction that may have taken place. Created films were ground in a Spex Cryomill for three 3 min cycles with a 1 min rest in between milling times. The ^{29}Si spectra (**Figures 7a-b**) correspond to PTESN and 20-CNC-PTESN. The 20-CNC-PTESN sample was chosen as it is the most likely to have a split peak in the ^{29}Si spectra indicating a possible hydrolysis or etherification reaction.[27] The neat PTESN sample was chosen as the control. The corresponding ^{13}C NMR (**Figure 7 c-d**) were present to verify agreement with the ^{29}Si NMR and note deviations from previous ^{13}C NMR scans of the monomeric species.[1]

Thermogravimetric Analysis

Thermogravimetric analysis (TGA) was carried out on a TA Instruments Q10 with a temperature ramp of 10 °C min^{-1} from room temperature to 1000 °C in nitrogen atmosphere for all composite samples. The raw CNC sample was equilibrated to 80 °C and held isothermally for 20 minutes to drive off residual moisture. The data from the TGA were then taken from the base weight at 80 °C and plotted in **Figure 6** in the relevant temperature range 80-600 °C.

Conclusions

Novel reinforced composites of PTESN and CNCs were cast from toluene. Though toluene is typically a poor solvent for CNC dispersion, we have shown that if PTESN is used as a polymer matrix, good CNC dispersion may be realized on both the macroscopic and nano scales. This is evidenced by the mechanical reinforcement observed through both tensile and DMA results, which show significant improvements at 5 wt% loading.[22] The higher thermal degradation temperature of the CNC as composites, as compared to the neat CNCs, suggests

CNCs in contact with alkoxysilanes can be melt processed into a variety of other silanes, opening these fillers up to use in a much larger variety of applications. This indicates the reported methods should allow lower melting point polymers of this type to be processed by extrusion, melt mixing and other conventional means leading to a new class of thermally stable CNC composite materials.

Conflicts of interest

The authors declare no conflict of interests.

Acknowledgements

The authors would like to acknowledge Christopher Winkler for operation of the JEOL 2100 TEM.

Notes and references

1. K. R. Gmernicki, E. Hong, C. R. Maroon, S. M. Mahurin, A. P. Sokolov, T. Saito and B. K. Long, ACS Macro Letters, 2016, **5**, 879-883.
2. B. J. Sundell, J. A. Lawrence Iii, D. J. Harrigan, J. T. Vaughn, T. S. Pilyugina and D. R. Smith, RSC Advances, 2016, **6**, 51619-51628.
3. M. V. Bermeshev, A. V. Syromolotov, L. E. Starannikova, M. L. Gringolts, V. G. Lakhtin, Y. P. Yampolskii and E. S. Finkelshtein, Macromolecules, 2013, **46**, 8973-8979.
4. J. Sapkota, M. Jorfi, C. Weder and E. J. Foster, Macromolecular rapid communications, 2014, **35**, 1747-1753.
5. J. Sapkota, J. C. Natterodt, A. Shirole, E. J. Foster and C. Weder, Macromolecular Materials and Engineering, 2017, **302**, 1600300-n/a.
6. M. V. Biyani, E. J. Foster and C. Weder, ACS Macro Letters, 2013, **2**, 236-240.
7. J. C. Natterodt, J. Sapkota, E. J. Foster and C. Weder, Biomacromolecules, 2017, **18**, 517-525.
8. V. Favier, J. Y. Cavaille, G. R. Canova and S. C. Shrivastava, Polymer Engineering & Science, 1997, **37**, 1732-1739.
9. A. Chakrabarty and Y. Teramoto, Polymers, 2018, **10**.
10. N. Belov, R. Nikiforov, L. Starannikova, K. R. Gmernicki, C. R. Maroon, B. K. Long, V. Shantarovich and Y. Yampolskii, European Polymer Journal, 2017, **93**, 602-611.
11. R. J. Moon, A. Martini, J. Nairn, J. Simonsen and J. Youngblood, Chemical Society Reviews, 2011, **40**, 3941-3994.
12. A. B. Elmabrouk, T. Wim, A. Dufresne and S. Boufi, Journal of Applied Polymer Science, 2009, **114**, 2946-2955.
13. A. B. Mabrouk, M. C. B. Salon, A. Magnin, M. N. Belgacem and S. Boufi, Colloids and Surfaces A: Physicochemical and Engineering Aspects, 2014, **448**, 1-8.
14. L. Yue, A. Maiorana, F. Khelifa, A. Patel, J. M. Raquez, L. Bonnaud, R. Gross, P. Dubois and I. Manas-Zloczower, Polymer, 2018, **134**, 155-162.
15. H. Kargarzadeh, R. M. Sheltami, I. Ahmad, I. Abdullah and A. Dufresne, Polymer, 2015, **56**, 346-357.
16. A. Ladhar, A. Ben Mabrouk, M. Arous, S. Boufi and A. Kallel, Polymer, 2017, **125**, 76-89.
17. A. Ladhar, M. Arous, S. Boufi and A. Kallel, Journal of Molecular Liquids, 2016, **224**, 515-525.
18. J. Yang, C.-R. Han, J.-F. Duan, M.-G. Ma, X.-M. Zhang, F. Xu, R.-C. Sun and X.-M. Xie, Journal of Materials Chemistry, 2012, **22**, 22467-22480.
19. J. Yang, C.-R. Han, J.-F. Duan, M.-G. Ma, X.-M. Zhang, F. Xu and R.-C. Sun, Cellulose, 2013, **20**, 227-237.
20. S. X. Peng, H. Chang, S. Kumar, R. J. Moon and J. P. Youngblood, Cellulose, 2016, **23**, 1825-1846.
21. L. Heux, G. Chauve and C. Bonini, Langmuir, 2000, **16**, 8210-8212.
22. E. J. Foster, R. J. Moon, U. P. Agarwal, M. J. Bortner, J. Bras, S. Camarero-Espinosa, K. J. Chan, M. J. D. Clift, E. D. Cranston, S. J. Eichhorn, D. M. Fox, W. Y. Hamad, L. Heux, B. Jean, M. Korey, W. Nieh, K. J. Ong, M. S. Reid, S. Renneckar, R. Roberts, J. A. Shatkin, J. Simonsen, K. Stinson-Bagby, N. Wanasekara and J. Youngblood, Chemical Society Reviews, 2018, **47**, 2609-2679.
23. A. Dufresne, Nanocellulose: from nature to high performance tailored materials, Walter de Gruyter GmbH & Co KG, 2017.
24. A. Bendahou, H. Kaddami and A. Dufresne, European Polymer Journal, 2010, **46**, 609-620.
25. M.-J. Cho and B.-D. Park, J. Ind. Eng. Chem., 2011, **17**, 36-40.
26. L. Pranger and R. Tannenbaum, Macromolecules, 2008, **41**, 8682-8687.
27. M.-C. B. Salon, G. Gerbaud, M. Abdelmouleh, C. Bruzzese, S. Boufi and M. N. Belgacem, Magnetic Resonance in Chemistry, 2007, **45**, 473-483.
28. H. Kono, S. Yunoki, T. Shikano, M. Fujiwara, T. Erata and M. Takai, Journal of the American Chemical Society, 2002, **124**, 7506-7511.

Supporting Information

Supporting information is available and includes **Figure S1** ^{1}H NMR of PTESN, **Figure S2** GPC data of PTESN, **Table S1** DMA data at various temperatures, **Table S2** tensile data, **Figure S3** representative tensile curves, **Figure S4** additional TGA traces, and **Figure S5** TEM of CNCs.

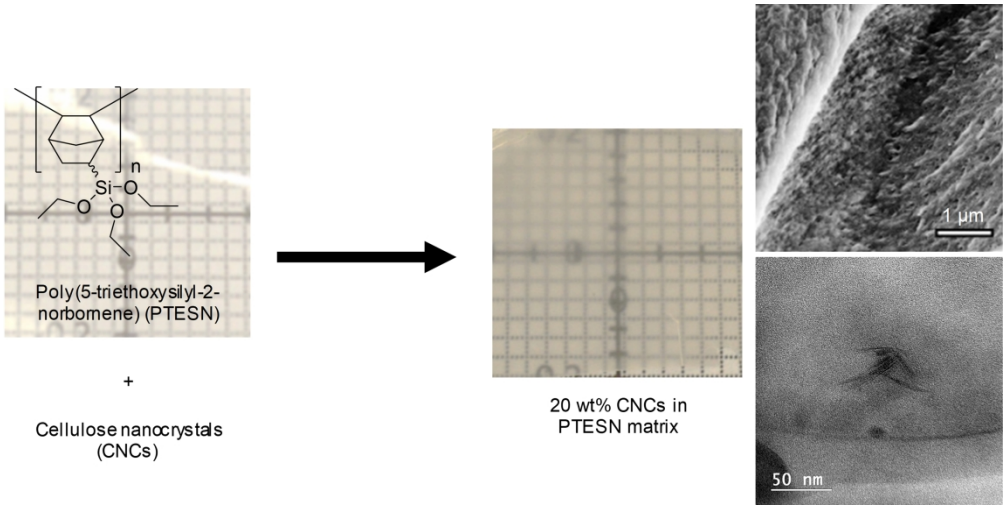

1422x711mm (96 x 96 DPI)